

Molar volume of solid isotopic helium mixtures

Carlos P. Herrero

Instituto de Ciencia de Materiales, Consejo Superior de Investigaciones Científicas (CSIC), Campus de Cantoblanco, 28049 Madrid, Spain

(Dated: October 25, 2018)

Solid isotopic helium mixtures have been studied by path-integral Monte Carlo simulations in the isothermal-isobaric ensemble. This method allowed us to study the molar volume as a function of temperature, pressure, and isotopic composition. At 25 K and 0.2 GPa, the relative difference between molar volumes of isotopically-pure crystals of ^3He and ^4He is found to be about 3%. This difference decreases under pressure, and for 12 GPa it is smaller than 1%. For isotopically-mixed crystals, a linear relation between lattice parameters and concentrations of helium isotopes is found, in agreement with Vegard's law. The virtual crystal approximation, valid for isotopic mixtures of heavier atoms, does not give reliable results for solid solutions of helium isotopes.

PACS numbers: 67.80.-s, 62.50.+p, 65.40.De, 05.10.Ln

I. INTRODUCTION

The lattice parameters of two chemically identical crystals with different isotopic composition are not equal, lighter isotopes giving rise to larger lattice parameters. This is due to the dependence of atomic vibrational amplitudes upon atomic mass, along with the anharmonicity of the vibrations. This effect is most important at low temperatures, since the zero-point amplitude decreases with increasing atomic mass. At higher temperatures, the isotope effect on the crystal volume is less relevant, and disappears in the high-temperature (classical) limit at $T > \Theta_D$ (Θ_D , Debye temperature), where vibrational amplitudes become independent of the atomic mass. At present, the isotopic effect in the lattice parameters of crystals can be measured with high precision¹.

Other quantities, such as the vibrational energy, display an isotope dependence at low T in a harmonic approximation, due to the usual rescaling of the phonon frequencies with the isotopic mass M ($\omega \propto M^{-1/2}$), but this dependence can show appreciable changes when anharmonic effects are present. All these effects are expected to be more important in the case of helium than for heavier atoms. In fact, solid helium is in many respects an archetypal “quantum solid,” where zero-point energy and associated anharmonic effects are appreciably larger than in most known solids. This gives rise to peculiar properties, whose understanding has presented a challenge for theories and modelling from a microscopic point of view².

Anharmonic effects in solids, and in solid helium in particular, have been studied theoretically for many years by using techniques such as quasiharmonic approximations and self-consistent phonon theories^{3,4,5}. An alternative procedure is based on the Feynman path-integral formulation of statistical mechanics^{6,7}, that has turned out to be a convenient approach to study thermodynamic properties of solids at temperatures lower than their Debye temperature Θ_D , where the quantum character of the atomic nuclei is relevant. In particular, Monte Carlo or molecular dynamics sampling can be applied to eval-

uate finite-temperature path integrals, thus allowing one to carry out quantitative and non-perturbative studies of anharmonic effects in solids².

The path-integral Monte Carlo (PIMC) method has been employed to study several structural and thermodynamic properties of solid helium^{2,8,9,10,11}, as well as heavier rare-gas solids^{12,13,14,15,16,17}. For helium, in particular, this procedure has predicted kinetic-energy values⁸ and Debye-Waller factors¹⁸ in good agreement with data derived from experiments^{19,20}. PIMC simulations have been also performed to study the isotopic shift in the helium melting pressure^{9,10}.

In most calculations of properties of crystals with isotopically mixed composition, it is usually assumed that each atomic nuclei in the solid has a mass equal to the average mass. This kind of *virtual-crystal approximation* has been used in density-functional calculations, as well as in PIMC simulations^{17,21,22,23,24,25}. In fact, in earlier simulations it was found that the results obtained by using this approximation are indistinguishable from those derived from simulations in which actual isotopic mixtures were considered. This seems to be true for atoms heavier than helium, and in particular for rare-gas solids including solid Ne¹⁷, but is not guaranteed to happen for solid helium, due to its low atomic mass and large anharmonicity.

It is well known that at temperatures lower than 1 K, a phase separation appears in solid ^3He - ^4He mixtures, and the actual temperature at which this separation occurs depends on pressure and isotopic composition^{26,27}. This isotope segregation is due to the different molar volume of both isotopes, which in turn is caused by the different zero-point vibrational amplitudes of ^3He and ^4He ^{27,28}. In this paper, we consider mixtures of helium isotopes at higher temperatures, where ^3He and ^4He form solid solutions for any isotopic composition. By varying the molar fraction of both isotopes, we analyze changes in the lattice parameter and kinetic energy, by using PIMC simulations. We employ the isothermal-isobaric (NPT) ensemble, which allows us to consider properties of these solid solutions along well-defined isobars. This simula-

tion method permits to study properties of actual isotopic mixtures, and compare them with those obtained for virtual crystals in which each atom has a mass equal to the average mass of the considered isotope mixture.

The paper is organized as follows. In Sec. II, the computational method is described. In Sec. III we present the results, and Sec. IV includes a discussion and the conclusions.

II. METHOD

Equilibrium properties of solid helium in the face-centred cubic (fcc) and hexagonal close-packed (hcp) phases have been calculated by PIMC simulations in the NPT ensemble. Our simulations were performed on supercells of the fcc and hcp unit cells, including 500 and 432 atoms respectively. These supercell sizes are enough for convergence of the quantities studied here²⁹. For a given average isotopic mass \bar{M} , we randomly distribute ^3He and ^4He atoms in the appropriate proportions over the lattice sites of the simulation cell, and the atoms are kept fixed at their respective positions along the simulation (no diffusive positional changes). This is assumed to be valid for the temperatures studied here, much higher than those at which phase separation appears ($T < 1$ K)^{26,27}. For each isotopic composition studied here, we have taken five different realizations of the isotope mixture. To analyze with more detail the dispersion in the lattice parameters obtained in the simulations, we took 12 different samples for $\bar{M} = 3.25$ amu, and 15 samples for $\bar{M} = 3.5$ amu (see below). For comparison, we have also considered virtual crystals, in which every atom has a mass \bar{M} , i.e., $M_i = \bar{M}$ for $i = 1, \dots, N$.

Helium atoms have been considered as quantum particles interacting through an effective interatomic potential, composed of a two-body and a three-body part. For the two-body interaction, we have taken the potential developed by Aziz *et al.*³⁰ (the so-called HFD-B3-FCII potential). For the three-body part we have employed a Bruch-McGee-type potential^{31,32}, with the parameters given by Loubeyre³², but with parameter A in the attractive exchange interaction rescaled by a factor $2/3$, as in Ref.¹⁰. This interatomic potential has been found to describe well the vibrational energy and equation-of-state of solid helium in the available range of experimental data, including pressures on the order of 50 GPa²⁹.

The PIMC method relies on an isomorphism between the considered quantum system and a classical one, obtained by replacing each quantum particle by a cyclic chain of N_{Tr} classical particles (N_{Tr} : Trotter number), connected by harmonic springs with a temperature-dependent constant. This isomorphism appears because of a discretization of the density matrix along cyclic paths, that is usual in the path-integral formulation of statistical mechanics^{6,7}. Details on this computational method can be found elsewhere^{2,33,34}.

Our simulations were based on the so-called “primi-

tive” form of PIMC^{35,36}. We considered explicitly two- and three-body terms in the simulations, which did not allow us to employ effective forms for the density matrix, developed to appreciably simplify the calculation when only two-body terms are explicitly considered¹⁰. Quantum exchange effects between atomic nuclei were not taken into account, since they are negligible for solid helium at the temperatures and pressures studied here. (This is expected to be valid as long as there are no vacancies and T is higher than the exchange frequency $\sim 10^{-6}$ K².) For the energy we have used the “crude” estimator, as defined in Refs.^{35,36}.

Sampling of the configuration space has been carried out by the Metropolis method at pressures $P \leq 12$ GPa, and temperatures between 10 K and the melting temperature at each considered pressure. However, most of the simulations presented in this paper were carried out for fcc He at 25 K and 0.3 GPa, conditions at which the isotopic effects studied here are clearly observable. Some simulations were also carried out at lower temperatures (see below). For given temperature and pressure, a typical run consisted of 10^4 Monte Carlo steps for system equilibration, followed by 10^5 steps for the calculation of ensemble average properties. To keep roughly constant the accuracy of the computed quantities at different temperatures, we have taken a Trotter number that scales as the inverse temperature $1/T$. At a given T , the value of N_{Tr} required to reach convergence of the results depends on the Debye temperature, higher Θ_D requiring larger N_{Tr} . Since vibrational frequencies increase as the applied pressure rises, N_{Tr} has to be raised accordingly. For pressures on the order of 1 GPa, $N_{Tr}T = 2000$ K is enough to reach convergence of the computed quantities. For pressures larger than 2 GPa, we have taken $N_{Tr}T = 4000$ K for ^3He and 3000 K for ^4He , as in earlier work²⁹. Other technical details are the same as those employed in Refs.^{16,29,37}.

In the isothermal-isobaric ensemble, the mean-square fluctuations in the volume V of the simulation cell are given by

$$\sigma_V^2 = \frac{V}{B} k_B T, \quad (1)$$

where $B = -V(\partial P/\partial V)_T$ is the isothermal bulk modulus³⁸. Hence, for a cubic crystal, the fluctuations in the lattice parameter a are:

$$\sigma_a^2 = \frac{k_B T}{9L^3 a B}, \quad (2)$$

where L^3 is the number of unit cells in a simulation cell with side length La . From Eq. (1) one can see that the relative fluctuation in the volume of the simulation cell, σ_V/V , scales as $L^{-3/2}$. For ^4He at 25 K we found in PIMC simulations $\sigma_V/V = 5.5 \times 10^{-3}$ for $P = 0.3$ GPa, and 1.7×10^{-3} for 12 GPa (for $L = 5$ and 500 atoms). For fcc ^4He at 0.3 GPa this translates into $\sigma_a = 7.3 \times 10^{-3}$ Å. We are interested in an accuracy in a on the order of 10^{-4} Å, which means that at this temperature and pressure

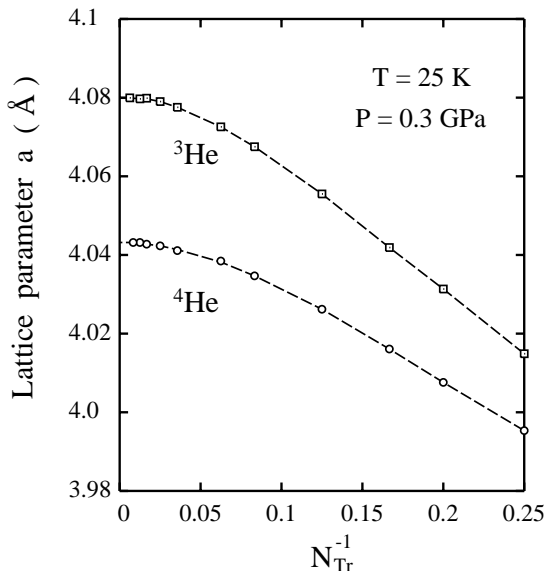


FIG. 1: Convergence of the lattice parameter a of fcc He as a function of the inverse Trotter number, N_{Tr}^{-1} , as derived from PIMC simulations at $T = 25$ K and $P = 0.3$ GPa. Squares and circles correspond to ^3He and ^4He , respectively. Dashed lines are guides to the eye. Error bars are smaller than the symbol size.

one needs about 10^4 independent data. In practice, the required number of Monte Carlo steps is expected to be larger, due to correlation between configurations along a Monte Carlo trajectory. In fact, we have checked that 10^5 Monte Carlo steps are enough to have an statistical uncertainty in a on the order of 10^{-4} Å.

III. RESULTS

We have checked the convergence with the Trotter number of several quantities derived from our PIMC simulations. In Fig. 1 we display the dependence of the lattice parameter a of fcc ^3He and ^4He , as a function of the inverse Trotter number N_{Tr}^{-1} , for $T = 25$ K and $P = 0.3$ GPa. The lattice parameter obtained in the simulations increases with N_{Tr} , and converges to a finite value for large N_{Tr} (limit $N_{Tr}^{-1} \rightarrow 0$ in Fig. 1). The difference $\delta a = a_3 - a_4$ between lattice parameters of ^3He and ^4He decreases as the Trotter number is lowered, and goes to zero in the classical limit ($N_{Tr} = 1$), where this isotopic effect disappears. The reliability of the interatomic potential employed here to predict lattice parameters of solid helium has been studied elsewhere²⁹. Here we will only comment that it gives good agreement with experimental results up to the melting temperature in the pressure range considered in this paper. Thus, for fcc ^4He at 38.5 K and 0.493 GPa we find $a = 3.9154$ Å vs 3.915(2) Å derived from inelastic neutron scattering³⁹.

Once checked its convergence with N_{Tr} , in Fig. 2 we show the temperature dependence of the lattice param-

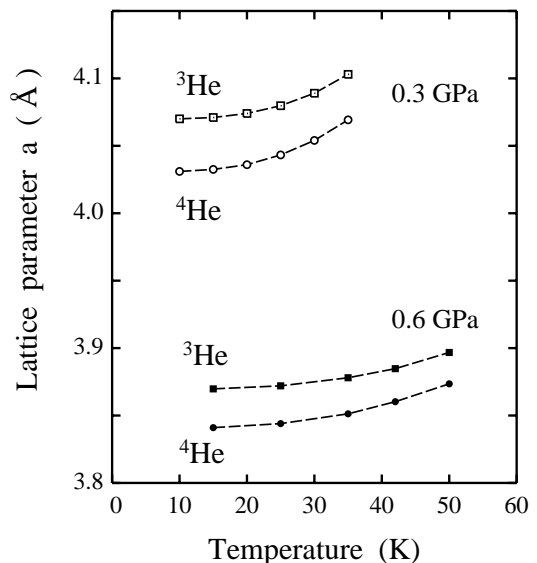


FIG. 2: Temperature dependence of the lattice parameter a of fcc helium, derived from PIMC simulations at two different pressures: 0.3 and 0.6 GPa. Squares and circles indicate results for ^3He and ^4He , respectively. Error bars are smaller than the symbol size. Dashed lines are guides to the eye.

eter a of fcc ^3He and ^4He at two different pressures: 0.3 GPa (open symbols) and 0.6 GPa (filled symbols). Squares correspond to ^3He and circles to ^4He . For each pressure, results are displayed for temperatures at which the considered solids were found to be stable along the PIMC simulations. As expected, a is larger for ^3He than for ^4He , and the difference $\delta a = a_3 - a_4$ is smaller for higher pressure. Also, for a given pressure, δa decreases slowly as the temperature is raised (at higher T the solid becomes “more classical”).

To quantify the change in crystal volume with isotopic mass, we calculate the ratio $\delta V/V_4 = (V_3 - V_4)/V_4$. This ratio is shown in Fig. 3 as a function of pressure for fcc (filled symbols) and hcp He (open symbols) at 25 K. At $P = 0.2$ GPa, we find $\delta V/V_4 = 0.030$. This value is reduced by more than a factor of 3 at $P = 12$ GPa, where we obtain $\delta V/V_4 = 7.7 \times 10^{-3}$. It is interesting to note that at $P = 1$ GPa, both fcc and hcp phases could be simulated at 25 K, remaining (meta)stable along the corresponding simulation runs. The ratio $\delta V/V_4$ obtained in both cases is shown in Fig. 3, and the results coincide within statistical errors. Direct experimental measurements of this isotopic effect on the molar volume are scarce. Stewart⁴⁰ measured the molar volumes of both ^3He and ^4He at 4.2 K and pressures up to 2 GPa. In particular, for $P = 0.3$ and 0.6 GPa he found $V_4/V_3 = 1.023$. At these pressures, we found for the low-temperature limit in the PIMC simulations $V_4/V_3 = 1.026(1)$ and $1.023(1)$, respectively.

The difference δV is largest at small pressures and low temperatures, where quantum effects are most important. For a given solid, quantum effects on the crystal volume can be measured by the difference $V - V_{c1}$ between

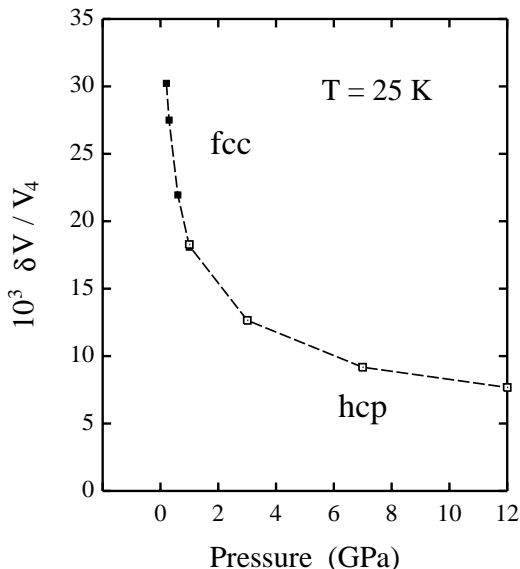


FIG. 3: Isotopic effect on the crystal volume of solid helium, as obtained from PIMC simulations. Shown is the ratio $\delta V/V_4 = (V_3 - V_4)/V_4$ as a function of pressure at 25 K. Open and filled symbols correspond to hcp and fcc phases, respectively. Error bars are less than the symbol size. The dashed line is a guide to the eye.

the actual volume V and that obtained for a “classical” crystal of point particles, V_{cl} . This difference decreases for increasing atomic mass and temperature^{13,41}. From our PIMC simulations at $T = 25$ K and a relatively low pressure of 0.3 GPa, we found an increase in the volume of solid ^3He and ^4He of 26% and 22% respectively, as compared to the “classical” crystal at zero temperature.

PIMC simulations allow us to obtain the kinetic energy of the different atoms in the simulation cell at finite temperatures. For pure fcc crystals of ^3He and ^4He , we find a kinetic energy $E_k = 9.22$ and 8.21 ± 0.03 meV/atom, respectively (at 25 K and 0.3 GPa). This translates into a kinetic-energy ratio of 1.12, slightly lower than the ratio between zero-point energies expected in a harmonic approximation ($E_0^3/E_0^4 = \sqrt{4/3} = 1.15$). These energy values are similar to those obtained earlier from PIMC simulations in the NVT ensemble. In particular, our results for ^4He (giving a molar volume of $9.95 \text{ cm}^3/\text{mol}$) are in line with those obtained earlier in the NVT ensemble at temperatures close to 25 K and molar volumes around $10 \text{ cm}^3/\text{mol}$ ¹⁸, which in turn agree with experimental measurements⁴².

For isotopically-mixed crystals, one expects the kinetic energy E_k of the whole crystal to evolve smoothly as a function of the mean isotopic mass \bar{M} . In Fig. 4 we show the kinetic energy of fcc helium vs \bar{M} at 25 K and 0.3 GPa, as derived from our PIMC simulations. Within the precision of our results, we observe a linear dependence of E_k vs \bar{M} , as indicated by the dashed line. We have compared these results with those obtained from PIMC simulations for the virtual crystal with mass \bar{M} ,

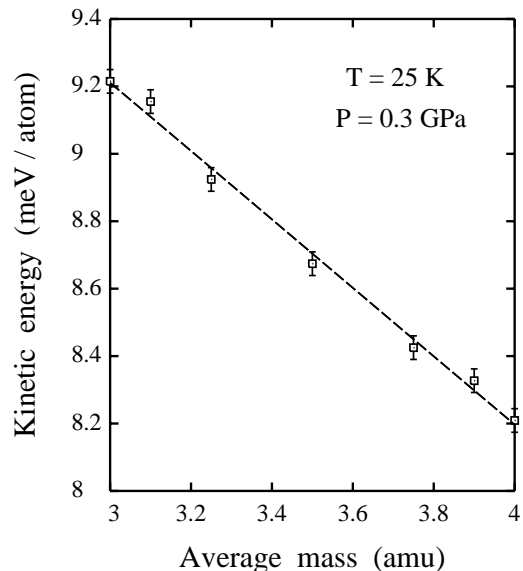


FIG. 4: Kinetic energy of fcc helium as a function of the mean isotopic mass \bar{M} in isotopically mixed crystals. Symbols are results of PIMC simulations at 25 K and 0.3 GPa. The dashed line is a linear fit to the data points.

and found that differences between both sets of results are smaller than the statistical noise. A discussion on the relation between vibrational kinetic and potential energies in solid helium was given elsewhere²⁹, and will not be repeated here.

Going back to the lattice parameter of fcc He, in Fig. 5 we display the dependence of a on the average isotopic mass, at 25 K and 0.3 GPa. Open squares correspond to simulations in which ^3He and ^4He atoms were randomly distributed over the crystal sites, according to the required average mass \bar{M} . The results show a linear dependence of a on \bar{M} . In Fig. 5 we also show results of PIMC simulations of fcc He, where each atom has a fictitious mass \bar{M} ($M_i = \bar{M}$ for $i = 1, \dots, N$). This virtual-crystal approximation yields for \bar{M} different from 3 and 4 amu a lattice parameter smaller than that obtained for a realistic distribution of isotopes over the simulation cell. For an isotopic mixture including 50% of each isotope, we find $a = 4.06162 \text{ \AA}$ vs $a_{vc} = 4.05950 \text{ \AA}$ for the virtual-crystal approximation, i.e., a difference between both models $a - a_{vc} = 2.12 \times 10^{-3} \text{ \AA}$. For this composition we have considered 15 different isotope distributions, and found for the lattice parameter a standard deviation $\sigma = 2.5 \times 10^{-4} \text{ \AA}$, a little smaller than the symbol size in Fig. 5. Thus, the difference $a - a_{vc}$ amounts to about 8σ . For 75% ^3He , we took 12 realizations of the isotope mixture, and found $a - a_{vc} = 1.64 \times 10^{-3} \text{ \AA}$. In this case, $\sigma = 2.8 \times 10^{-4} \text{ \AA}$, or $a - a_{vc} \approx 6\sigma$.

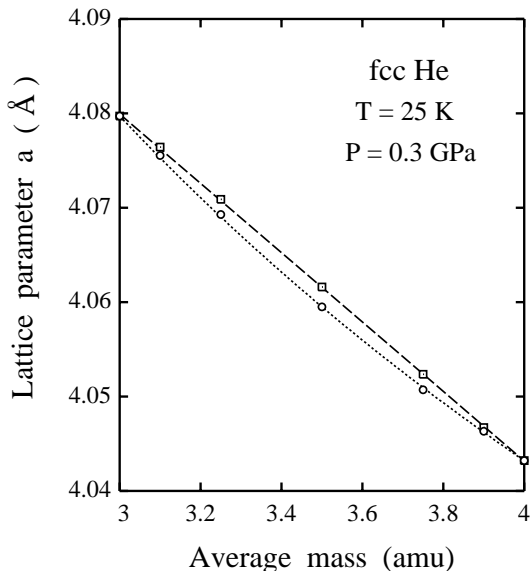


FIG. 5: Lattice parameter a of fcc helium as a function of the mean isotopic mass \overline{M} . Data points were obtained from PIMC simulations at 25 K and 0.3 GPa, for isotopically mixed crystals containing ^3He and ^4He (squares), and for virtual crystals built up by atoms with the average isotopic mass (circles). Error bars are smaller than the symbol size. The dashed line is a least-square fit to the data points (squares). The dotted line was obtained from a quasi-harmonic approximation using Eq. (5).

IV. DISCUSSION

Path-integral Monte Carlo simulations have been found to be well suited to study finite-temperature anharmonic effects on structural and thermodynamic properties of crystalline solids. These effects are particularly important for solid helium, where isotopic effects are relevant, as manifested in differences in the molar volume and vibrational energies of solid ^3He and ^4He . The PIMC method enables us to study phonon-related properties without the assumptions of quasiharmonic or self-consistent phonon approximations, and to study anharmonic effects in solids in a non-perturbative way. Thus, for a given reliable interatomic potential, this method yields in principle “exact” values for measurable properties of many-body quantum problems, with an accuracy limited by the imaginary-time step (Trotter number) and the statistical uncertainty of the Monte Carlo sampling.

Our results for the lattice parameter of solid helium as a function of the average isotopic mass (see Fig. 5) can be understood in terms of the theory of alloys. In fact, ^3He and ^4He behave in this respect as atoms with different atomic radii, as a consequence of the different vibrational amplitudes of both isotopes. If we consider a ^4He crystal with ^3He impurities, the lattice expansion Δa due to these impurities is given by Vegard’s law^{43,44}:

$$\frac{\Delta a}{a_4} = \beta C_3, \quad (3)$$

where C_3 is the concentration of ^3He . From the data presented in Fig. 5 we find an expansion coefficient $\beta = 1.49 \times 10^{-25} \text{ cm}^3/\text{atom}$. According to our results, this linear relation between lattice parameter and isotope concentration holds for the whole concentration range, as shown in Fig. 5 (squares and dashed line). This is in agreement with earlier calculations for alloys, which indicate that for a difference between atomic radii less than $\sim 5\%$ one does not expect appreciable departure from linearity⁴⁴. In fact, ^3He and ^4He behave as atoms with a difference in effective atomic radii of about 1% (for T and P considered here).

The virtual-crystal approximation has been employed earlier to study the dependence of lattice parameters on the average isotopic mass. This can be conveniently done by using a quasiharmonic approach, according to which the low-temperature lattice parameter a for mean isotopic mass \overline{M} can be approximated by²¹

$$a = a_\infty + \frac{1}{6Ba_\infty^2} \sum_{n,\mathbf{q}} \hbar\omega_n(\mathbf{q})\gamma_n(\mathbf{q}). \quad (4)$$

Here, $\omega_n(\mathbf{q})$ are the frequencies of the n th mode in the crystal, B is the bulk modulus, a_∞ is the zero-temperature lattice constant in the limit of infinite atomic mass (classical limit), and $\gamma_n(\mathbf{q}) = -\partial \ln \omega_n(\mathbf{q}) / \partial \ln V$ is the Grüneisen parameter of mode n, \mathbf{q} . Assuming a mass dependence of the frequencies $\omega_n(\mathbf{q}) \sim \overline{M}^{-1/2}$, one finds for the relative change in lattice parameter with isotopic mass

$$a \approx a_\infty + A\overline{M}^{-\frac{1}{2}}, \quad (5)$$

where A is constant for a given pressure. By applying this equation to a_3 and a_4 , we can find A , and then the dependence of a on \overline{M} shown in Fig. 5 as a dotted line. This line coincides within error bars with the results derived from the PIMC simulations for helium with $M_i = \overline{M}$ for all i (virtual crystal). Note that the low-temperature expression for the lattice parameter given in Eq. (4) is a good approximation for the conditions (P, T) considered here. In fact, for a volume of $\sim 10 \text{ cm}^3/\text{mole}$, a temperature of 25 K can be considered a “low temperature” when compared with $\Theta_D \gtrsim 120 \text{ K}$ ¹⁹.

It is worth commenting on the difference found between this quasiharmonic approximation and the actual isotope distribution over the crystal. For the virtual crystal we found in both PIMC simulations and in the quasiharmonic approach, a non-linear dependence of the lattice parameter a on average isotopic mass. This contrasts with the linear dependence derived from PIMC simulations for actual distributions of isotopes. (If a departure from linearity appears in this case, it will be smaller than the precision of our results.) This observation is important for the helium solid solutions considered here, since in most known solids both approaches give the same results^{17,21,25}. From the results displayed in Fig. 5, we observe for $\overline{M} = 3.5 \text{ amu}$ a difference $a - a_{vc} = 2.1 \times 10^{-3}$

Å, which amounts to about 0.05% of the lattice parameter. This relative difference is much larger than the uncertainty in structural parameters currently derived from diffraction methods¹.

In the last few years, several authors have indicated that pressure causes a decrease in anharmonicity^{45,46,47}, in agreement with earlier observations that the accuracy of quasiharmonic approximations increases as pressure is raised and the density of the solid increases^{48,49}. This is also the origin of the decrease in the isotopic effects studied here, as pressure is raised. Since these isotopic effects are caused by anharmonicity of the interatomic interactions, an effective decrease in anharmonicity causes a reduction in the difference $\delta a = a_3 - a_4$ or, equivalently, in the ratio $\delta V/V_4$ shown in Fig. 3.

In summary, we have carried out PIMC simulations of solid solutions of helium isotopes in the isothermal-isobaric ensemble. Our results indicate that Vegard's law

is fulfilled in the whole composition range, i.e., the crystal volume changes linearly with isotopic composition. This volume change decreases appreciably as pressure is raised, but it is still clearly observable at pressures of the order of 10 GPa. Approximations such as virtual crystals with average atomic mass are not valid for solid isotopic helium mixtures.

Acknowledgments

The author benefitted from discussions with R. Ramírez. This work was supported by Ministerio de Educación y Ciencia (Spain) through Grant No. FIS2006-12117-C04-03.

-
- ¹ A. Kazimirov, J. Zegenhagen, and M. Cardona, *Science* **282**, 930 (1998).
 - ² D. M. Ceperley, *Rev. Mod. Phys.* **67**, 279 (1995).
 - ³ M. L. Klein and J. A. Venables, eds., *Rare Gas Solids* (Academic Press, New York, 1976).
 - ⁴ G. P. Srivastava, *The Physics of Phonons* (Adam Hilger, Bristol, 1990).
 - ⁵ R. G. D. Valle and E. Venuti, *Phys. Rev. B* **58**, 206 (1998).
 - ⁶ R. P. Feynman, *Statistical Mechanics* (Addison-Wesley, New York, 1972).
 - ⁷ H. Kleinert, *Path Integrals in Quantum Mechanics, Statistics and Polymer Physics* (World Scientific, Singapore, 1990).
 - ⁸ D. M. Ceperley, R. O. Simmons, and R. C. Blasdel, *Phys. Rev. Lett.* **77**, 115 (1996).
 - ⁹ J. L. Barrat, P. Loubeyre, and M. L. Klein, *J. Chem. Phys.* **90**, 5644 (1989).
 - ¹⁰ M. Boninsegni, C. Pierleoni, and D. M. Ceperley, *Phys. Rev. Lett.* **72**, 1854 (1994).
 - ¹¹ S. Y. Chang and M. Boninsegni, *J. Chem. Phys.* **115**, 2629 (2001).
 - ¹² A. Cuccoli, A. Macchi, V. Tognetti, and R. Vaia, *Phys. Rev. B* **47**, 14923 (1993).
 - ¹³ M. H. Müser, P. Nielaba, and K. Binder, *Phys. Rev. B* **51**, 2723 (1995).
 - ¹⁴ C. Chakravarty, *J. Chem. Phys.* **116**, 8938 (2002).
 - ¹⁵ M. Neumann and M. Zoppi, *Phys. Rev. E* **65**, 031203 (2002).
 - ¹⁶ C. P. Herrero, *Phys. Rev. B* **65**, 014112 (2002).
 - ¹⁷ C. P. Herrero, *J. Phys.: Condens. Matter* **15**, 475 (2003).
 - ¹⁸ E. W. Draeger and D. M. Ceperley, *Phys. Rev. B* **61**, 12094 (2000).
 - ¹⁹ D. A. Arms, R. S. Shah, and R. O. Simmons, *Phys. Rev. B* **67**, 094303 (2003).
 - ²⁰ C. T. Venkataraman and R. O. Simmons, *Phys. Rev. B* **68**, 224303 (2003).
 - ²¹ A. Debernardi and M. Cardona, *Phys. Rev. B* **54**, 11305 (1996).
 - ²² M. Cardona, *Phys. Status Solidi (b)* **220**, 5 (2000).
 - ²³ A. P. Zhernov, *Low Temp. Phys.* **26**, 908 (2000).
 - ²⁴ C. P. Herrero, *Phys. Status Solidi B* **220**, 857 (2000).
 - ²⁵ C. P. Herrero, *J. Phys.: Condens. Matter* **13**, 5127 (2001).
 - ²⁶ R. H. Arnold and P. B. Pipes, *Phys. Rev. B* **21**, 5156 (1980).
 - ²⁷ N. Sullivan and A. Landesman, *Phys. Rev. B* **25**, 3396 (1982).
 - ²⁸ W. J. Mullin, *Phys. Rev. Lett.* **20**, 254 (1968).
 - ²⁹ C. P. Herrero, *J. Phys.: Condens. Matter* **18**, 3469 (2006).
 - ³⁰ R. A. Aziz, A. R. Janzen, and M. R. Moldover, *Phys. Rev. Lett.* **74**, 1586 (1995).
 - ³¹ L. W. Bruch and I. J. McGee, *J. Chem. Phys.* **59**, 409 (1973).
 - ³² P. Loubeyre, *Phys. Rev. Lett.* **58**, 1857 (1987).
 - ³³ M. J. Gillan, *Phil. Mag. A* **58**, 257 (1988).
 - ³⁴ J. C. Noya, C. P. Herrero, and R. Ramírez, *Phys. Rev. B* **53**, 9869 (1996).
 - ³⁵ D. Chandler and P. G. Wolynes, *J. Chem. Phys.* **74**, 4078 (1981).
 - ³⁶ K. Singer and W. Smith, *Mol. Phys.* **64**, 1215 (1988).
 - ³⁷ J. C. Noya, C. P. Herrero, and R. Ramírez, *Phys. Rev. B* **56**, 237 (1997).
 - ³⁸ L. D. Landau and E. M. Lifshitz, *Statistical Physics* (Pergamon, Oxford, 1980), 3rd ed.
 - ³⁹ W. Thomlinson, J. Eckert, and G. Shirane, *Phys. Rev. B* **18**, 1120 (1978).
 - ⁴⁰ J. W. Stewart, *Phys. Rev.* **129**, 1950 (1963).
 - ⁴¹ C. P. Herrero and R. Ramírez, *Phys. Rev. B* **63**, 024103 (2001).
 - ⁴² S. O. Diallo, J. V. Pearce, R. T. Azuah, and H. R. Glyde, *Phys. Rev. Lett.* **93**, 075301 (2004).
 - ⁴³ L. Vegard, *Z. Phys.* **5**, 17 (1921).
 - ⁴⁴ A. R. Denton and N. W. Ashcroft, *Phys. Rev. A* **43**, 3161 (1991).
 - ⁴⁵ A. I. Karasevskii and W. B. Holzapfel, *Phys. Rev. B* **67**, 224301 (2003).
 - ⁴⁶ H. M. Lawler, E. K. Chang, and E. L. Shirley, *Phys. Rev. B* **69**, 174104 (2004).
 - ⁴⁷ C. P. Herrero and R. Ramírez, *Phys. Rev. B* **71**, 174111 (2005).
 - ⁴⁸ E. L. Pollock, T. A. Bruce, G. V. Chester, and J. A.

Krumhansl, Phys. Rev. B **5**, 4180 (1972).
⁴⁹ B. L. Holian, W. D. Gwinn, A. C. Luntz, and B. J. Alder,

J. Chem. Phys. **59**, 5444 (1973).